Flexoelectricity in a metal/ferroelectric/semiconductor heterostructure

Shujin Huang, Hei-Man Yau, Hyeonggeun Yu, Lu Qi, Franky So, Ji-Yan Dai, and Xiaoning Jiang

---

Flexoelectricity in a metal/ferroelectric/semiconductor heterostructure

Shujin Huang,[1] Hei-Man Yau,[2] Hyeonggeun Yu,[3] Lu Qi,[1] Franky So,[3] Ji-Yan Dai,[2] and Xiaoning Jiang[1,a]

[1]*Department of Mechanical and Aerospace Engineering, North Carolina State University, Raleigh, NC 27695, U.S.A*

[2]*Department of Applied Physics, The Hong Kong Polytechnic University, Hung Hom, Kowloon, Hong Kong, China*

[3]*Department of Material Science and Engineering, North Carolina State University, Raleigh, NC 27695, U.S.A*

The flexoelectricity in a 100 nm-thick BaTiO$_3$ (BTO) thin film based metal/ferroelectric insulator/semiconductor (MFS) heterostructure was reported in this letter. The transverse flexoelectric coefficient of the BTO thin film in the hetero-junction structure was measured to be 287-418 μC/m at room temperature, and its temperature dependence shows that the flexoelectric effect in the BTO thin film was dominated in the paraelectric phase. We showed that the BTO thin film capacitance could be controlled at multi-levels by introducing ferroelectric and flexoelectric polarization in the film. These results are promising for understanding of the flexoelectricity in epitaxial ferroelectric thin films and practical applications of the enhanced flexo-electricity in nanoscale devices. *© 2018 Author(s). All article content, except where otherwise noted, is licensed under a Creative Commons Attribution (CC BY) license (http://creativecommons.org/licenses/by/4.0/).* https://doi.org/10.1063/1.5031162

Flexoelectric effect refers to electromechanical coupling due to electric polarization and strain gradient, which was first proposed by Kogan in the 1960s.[1] It has earned growing research attention in recent years, as a possible substitution for piezoelectricity.

Flexoelectricity is defined as[2,3]

$$P_i = \mu_{ijkl}\frac{\partial \varepsilon_{jk}}{\partial x_l}, \tag{1}$$

where P_i is the induced polarization; μ_{ijkl} is the flexoelectric coefficient; and ε_{jk} is the applied strain. Unlike piezoelectricity which only exists in ferroelectric phases of non-centrosymmetric materials, flexoelectricity is a universal effect existing in all materials at both ferroelectric and para-electric phases. Tagantsev estimated the flexoelectric coefficient to be proportional to *ke/a*, where *k* is the dielectric constant and *e/a* is the ratio of the ionic charge to the lattice constant,[3,4] suggesting that oxide ferroelectrics with large dielectric constants could be promising flexoelectric materials.

Flexoelectricity has been mostly reported for insulating ferroelectric materials such as BaTiO$_3$, SrTiO$_3$, BST, BT-8BST, SrTiO$_3$, PMN-PT and polyvinylidene fluoride (PVDF).[5–14] Recently, it was found that some semiconducting materials can also yield polarization upon strain gradients. Catalan's group has demonstrated that the effective flexoelectric coefficient of oxygen depleted BaTiO$_3$ (BTO$_{-\delta}$) can reach up to 1 *mC/m*.[6] Due to the oxygen depletion process, BaTiO$_3$ (BTO) became an n-type semiconductor where the surface was fully oxidized and capped by the thin insulating layer. The enhanced flexoelectricity was induced by the surface reduced layer, where the strong electric field was generated in the semiconducting BTO$_{-\delta}$ under strain gradients.

---

[a]Electronic Email: xjiang5@ncsu.edu

Since the flexoelectric effect is expected to be more significant when the material is shrunk down to the nanoscale due to its scaling effect,[15] the flexoelectric effects in ferroelectric thin films have attracted a lot of attentions.[16] However, most of the reported studies focused on the flexo-electric effect in single ferroelectric thin films epitaxially grown on a lattice-matching substrate. More recently, extremely thin flexoelectric films have been explored showing promising flexoelec-tricity.[17] Given that the ferroelectric thin film devices such as ferroelectric field-effect transistors[18] or ferroelectric tunnel junction memories[19] require multi-layered film structure, investigating the flexoelectric effect in ferroelectric hetero-junctions is important.[20,21] Particularly, an interesting thin film based multilayer structure, metal/ferroelectric insulator/semiconductor (MFS) hetero-structure exploiting the ferroelectric tunnel junctions (FTJs), has been extensively studied for a resistive switching memory.[19,22–24] Although the ferroelectric-induced tunneling has been demonstrated exper-imentally as the dominated transport mechanism in FTJs, it was not clear whether flexoelectricity played a role in the mechanism of resistive switching memory or not. It is worth to mention that the theoretical mechanism of flexoelectric impacts on ferroelectric switching was predicted using the Landau–Ginsburg–Devonshire phenomenological approach.[25,26] When the external elec-trical field applied on the bending beam, the energy profile of the BTO thin film (20 nm) can be recovered. Thus, they predicted the switching mechanism in the epitaxial grown ferroelectric thin film.

In this work, an experimental study on the flexoelectricity in Pt/BTO/Nb-doped SrTiO3 (MFS) heterojunctions is presented. A layer of 100 nm-thick BTO epitaxial thin film deposited on Nb 0.7wt% doped $SrTiO_3$ (Nb:STO) substrate was prepared for the MFS heterojunction and the flexoelectric coefficient of the BTO thin film was then extracted. A ferroelectric tunnel junction (FTJ) was formed by poling the BTO layer, resulting in a resistive switching memory. The flexoelectricity in the BTO thin film harnessed with the ferroelectricity was then studied to control multi-level polarization of the BTO thin film.

A metal/ferroelectric/semiconductor heterostructure was prepared for electrical polarization tests (Fig. 1). A layer of 100-nm-thick BTO thin film was deposited epitaxially on a [001]-oriented single-crystalline 0.7wt% Nb-doped SrTiO3 (Nb:STO, n-type) substrate by pulsed-laser deposition in a typical epitaxial growth mode.[24] 30 nm thick Pt top electrodes were then sputtered onto BTO/Nb:STO with a dot patterned mask to form the MFS heterostructure. Besides, indium electrode and Au elec-trode were pressed and sputtered to the structure, respectively, to ensure an ohmic contact formed with Nb:STO. The electrical output induced by mechanical bending within the MFS was monitored through a pair of wires connected to the Pt electrode and the Indium ohmic contact pad on the Nb:STO substrate.

Another pair of wire connections were made between the indium ohmic contact and the evap-orated Au electrode on the bottom side of Nb:STO substrate, which will be used to monitor the electrical response induced purely from the Nb:STO substrate upon mechanical bending.

Fig. 2 shows the schematic diagram of the electrical polarization measurements. The MFS structured beam was clamped rigidly at one end and deflected at the other end by a piezoelectric
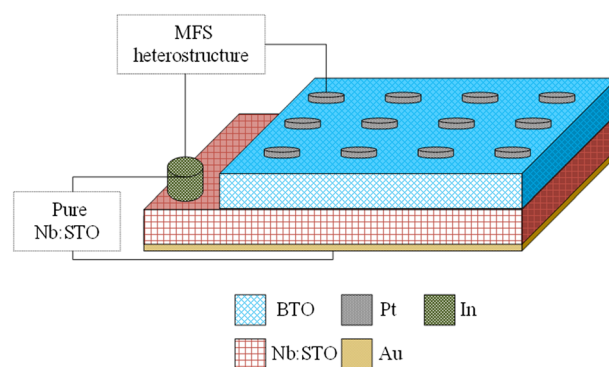
FIG. 1. Schematic illustration of the Pt/BTO/Nb:STO metal/ferroelectric/semiconductor heterostructure.
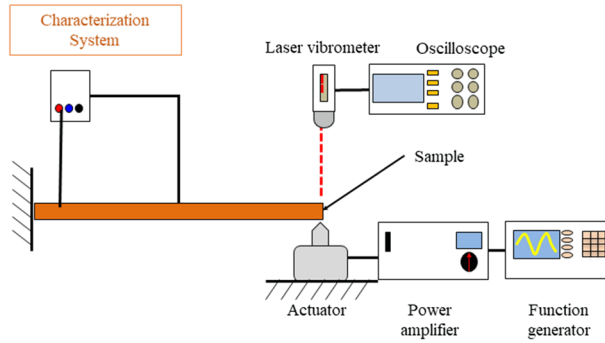
FIG. 2. The experimental set-up for electrical polarization measurement.

actuator, which was driven by a function generator (Tektronix Model AFG3101) at an excitation frequency of 10 Hz along with a power amplifier (Brüel & Kjær, type 2706, Nærum, Denmark). The displacement of the deflected end was measured using a laser vibrometer (Polytec, OFV-5000), which was connected to an oscilloscope (Agilent model DSO7104B). For a simple cantilever, the induced electrical polarization is represented by:

$$P_3 = \mu_{12} \frac{\partial \varepsilon_{xx}}{\partial x_z} + d_{31} \varepsilon_{xx} + P_s, \tag{2}$$

where the first term is the flexoelectric polarization, the second term is the piezoelectric polarization and the last term is the ferroelectric polarization. To achieve the controllably bending in two opposite directions, the same displacement of the deflected end was reached by monitoring through the laser vibrometer.

A lock-in amplifier (Stanford Research System Model SR830) was used to record the electrical polarization current induced by bending, for both sets of electrodes. A semiconductor characterization system (Keneith model 4200-SCS) was used to record the capacitance change of the MFS structure upon bending. Similar tests were also conducted at elevated temperatures using a set-up described in our previous work.[27] The temperature range was set to be between 70 °C and 160 °C.

In order to understand the polarization in the MFS structure, three effects were examined here: the ferroelectricity, the piezoelectricity and the flexoelectricity. The deflected end of the samples was vibrated in two directions as shown in Fig. 3. The sample was poled before the bending test and the corresponding ferroelectric polarization direction is marked as the red arrow. The directions of induced flexoelectric (blue arrow) and piezoelectric polarizations (green arrow) are also marked according to the bending direction. Therefore, four different polarization states are demonstrated by combining ferroelectric, piezoelectric and flexoelectric polarization as shown in Fig. 3.

To determine the ferroelectric polarization of the MFS structure, the resistance switching effect was tested by measuring current change when external pulsed-train writing voltages were used in the sequence illustrated with a step of 0.2 V, and the read voltage remained unchanged as $V_{read} = 0.5$ V. The positive voltage pulse drives the BTO polarization pointing to NSTO electrode and sets the junction to the ON state (the voltage is applied on the top electrode while the bottom electrode is grounded). The Pt/BTO/NSTO device is set to the OFF state by applying a negative pulse, which switches the polarization towards the Pt electrode. The results, as shown in Fig. 4, suggest that the resistance can be varied by applying an external electric field. By sweeping the writing voltage from 8 V to -10 V, two resistance states are obtained. A low resistance state (LRS) is obtained when a positive voltage (8 V) is applied to the Pt electrode while a high resistance state (HRS) is achieved when -10 V is applied. Fig. 4 shows the two distinct current states obtained at 0.5 V after poling the ferroelectric layer at positive (red) and negative (black) voltages, which confirms the non-volatile resistance switching of the MFS heterojunction.[24]

Apart from the ferroelectric effect, the piezoelectric response was checked by measuring the d_{33} value via the piezoelectric d_{33} meter (Institute of Acoustics Academia Sinica, Model ZJ-3D). The observed d_{33} (the effective d_{33}) was weaker than 1 pC/N, which can be converted into the d_{31}.
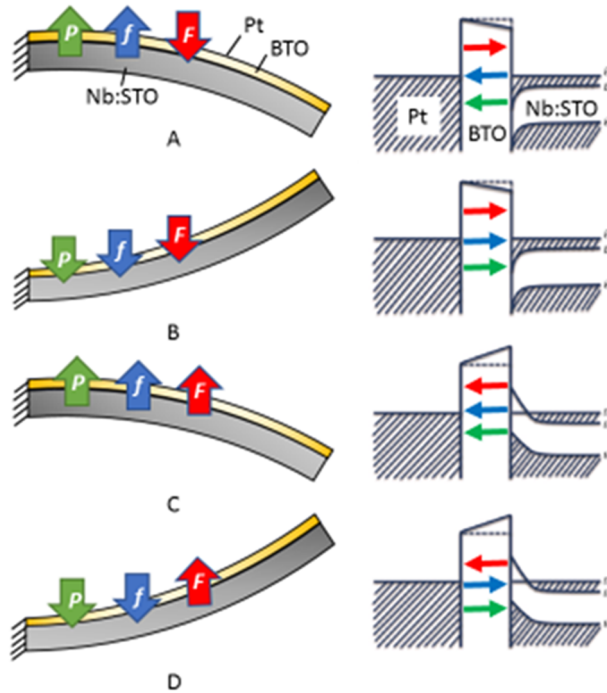
FIG. 3. Schematic description of the polarization directions induced by bending the sample or by applying an electric field, and the corresponding band diagrams of the MFS structure. (A) & (B): The ferroelectric layer is poled as low resistance state by applying a positive voltage (8 V) to the Pt electrode; (C) & (D): the ferroelectric layer is poled as high resistance state by applying a negative voltage (-10 V). The mechanical bending direction is shown as the beam deformation. The blue, red, and green arrows denote the flexoelectric, ferroelectric and piezoelectric polarization direction, respectively. A rectangular barrier in the band diagram, denoted by the dashed and solid lines, is assumed before and after the ferroelectric layer is poled, respectively. The arrow in the barrier indicates the dipole induced by ferroelectric (red), flexoelectric (blue), piezoelectric (green), respectively.

The d_{31} is proportional to the effective d_{33} with the square of the length-to-thickness ratio. Since the length-to-thickness ratio of the BTO thin film is in the order of 10^5, the transverse piezoelectric coefficient d_{31} is extremely small (ten orders smaller than the effective d_{33}).[15] Thus, the piezoelectric polarization was neglected throughout the experiment. Fig. 5(a) shows the polarization in the MFS structure as function of a strain gradient. The strain gradient was calculated from the Euler-Bernoulli beam theory.[28] It is worth to note the lattice mismatch between BTO thin film and Nb:STO substrate, which can cause the inhomogeneous in-plane strain inside of BTO thin film.[29] Further discussion will
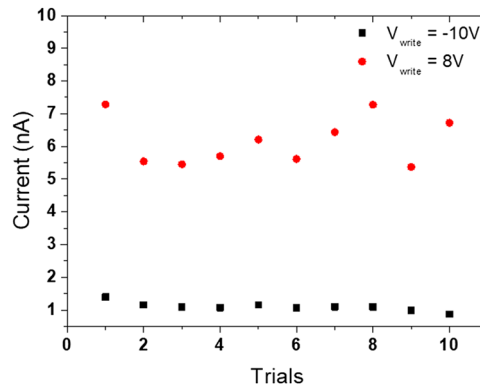
FIG. 4. Current-voltage characteristics of MFS structure before bending.
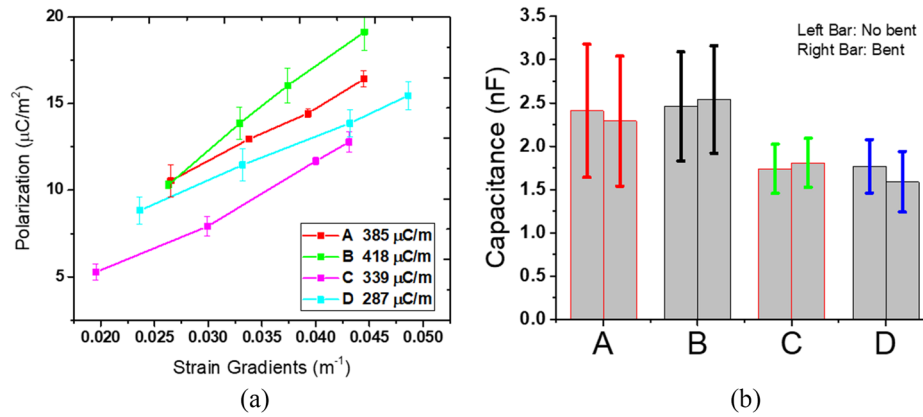
FIG. 5. (a) Induced polarization as a function of strain gradients, and (b) the capacitance for the four different states induced by combining the ferroelectric polarization with the flexoelectric polarization. The error bars in (b) are added under a calculation of capacitance for 4 samples. A, B, C and D indicate four different combination of polarizations in Fig. 3 accordingly.

be included later in the paper. The polarization induced mechanical deflection is linearly proportional to the strain gradient, where the slope indicates the effective flexoelectric coefficient. The estimated (Slope) is ~385 µC/m for Case A, ~418 µC/m for Case B, ~339 µC/m for Case C and ~287 µC/m for Case D. This phenomenon agrees with the analysis of the dipole distributions shown in Fig. 3. It is worth noted that for Case A and C, or for Case B and D, the MFS structure was set at LRS and HRS, respectively. Even though the mechanical bending direction is the same, the flexoelectric coefficients were different due to the ferroelectric polarization from a capacitor.

To understand the different polarization states and interpret the variation of flexoelectric coefficients, the capacitance of the MFS structure for the four different cases (A,B,C, and D) was measured under an accumulation mode (positive bias applied to the Pt electrode) as shown in Fig. 5(b). In case of B and C, the directions of the ferroelectric and flexoelectric polarization are same so that the dipoles were lined up in the same direction as shown in Figure 3 and hence the capacitance should increase after the bending. In case of A and D, on the other hand, the directions of the ferroelectric and flexoelectric polarization are opposite. The polarization induced by the flexoelectricity compensates the one induced by the ferroelectricity and hence the capacitance decreases after the bending. It is noted that the absolute capacitance for LRS (A and B) is larger than the capacitance for HRS (C and D). Under HRS (C and D), the ferroelectric polarization in the BTO thin film induces a depleted Nb:STO region at the BTO/Nb:STO interface as shown in the band diagram in Figure 3. Hence, the total capacitance of the MFS structure is described as:

$$\frac{1}{C_{BTO}} + \frac{1}{C_{Nb:STO}} = \frac{1}{C_{Total}},$$

where the C_{BTO} is the capacitance in the BTO thin film, $C_{Nb:STO}$ is the capacitance in the Nb:STO substrate, and C_{Total} is the total capacitance in the MFS structure. In case of LRS (A and B), the ferroelectric polarization in the BTO thin film attracts the majority carriers in the Nb:STO to the BTO/Nb:STO interface as shown in the band diagram (Figure 3). Hence, $C_{Nb:STO}$ is negligible and the total capacitance is larger compared to the cases for HRS (C and D) as shown in Fig. 5(b). As a result of the combined effects of resistance states and bending directions, four different capacitance levels could be demonstrated.

In addition, the bending experiment was performed as a function of temperature from 70°C to 160°C. The transverse flexoelectric coefficient of the MFS structure with different poling directions are shown in Fig. 6. With the Curie temperature at 120 °C, the flexoelectricity exists in both ferroelectric phase and paraelectric phase, while the ferroelectricity only exists in the ferroelectric phase. Therefore, above the Curie temperature, the crystalline structure of BTO thin film transformed into paraelectric phase so that the ferroelectric effect was gradually eliminated. The flexoelectric effect
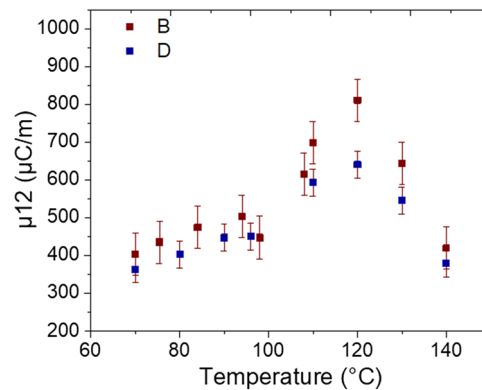
FIG. 6. Temperature dependence of the transverse flexoelectric coefficient of MFS Structure with two different poling directions.

is dominated in the paraelectric phase so that the effective flexoelectric coefficients of B and D can gradually fall as the same actual flexoelectric coefficient.

To investigate more about the flexoelectricity in such structure, a few more tasks still need to be addressed. One is to measure the longitudinal flexoelectric coefficient, which would not only complete the study of the flexoelectricity in the ferroelectric thin film, but also would help to understand the build-in strain distribution and contribution to the flexoelectric response. When the thickness of ferroelectric thin film is down to tens or several nanometers, the lattice mismatch would induced larger in-plane strain. Therefore, the thickness dependence study is the other interesting related topic since it can influence both the capacitance of the ferroelectric thin film layer and the strain distribution. Also, it would be interesting to investigate whether the thin film can obey the scaling effect at a thickness of a few unit cells.

In conclusion, the flexoelectric coefficient of BTO thin films with a MFS structure was characterized using the cantilever bending method over a temperature range from 70°C to 160°C. Our work demonstrated that the flexoelectric polarization of the Pt/BTO/Nb:STO MFS structure is purely generated from the BTO thin film layer. Multi-level control of the capacitance in the MFS structure was achieved by combining both ferroelectric and flexoelectric polarizations.

[1] S. M. Kogan, Sov. Physics-Solid State **5**, 2069 (1964).
[2] V. L. Indenbom, E. B. Loginov, and M. A. Osipov, Kristallografiya **26**, 1157 (1981).
[3] A. K. Tagantsev, Phys. Rev. B **34**, 5883 (1986).
[4] P. Zubko, G. Catalan, and A. K. Tagantsev, Annu. Rev. Mater. Res. **43**, 387 (2013).
[5] U. K. Bhaskar, N. Banerjee, A. Abdollahi, Z. Wang, D. G. Schlom, G. Rijnders, and G. Catalan, Nat. Nanotechnol. **11**, 263 (2016).
[6] J. Narvaez, F. Vasquez-Sancho, and G. Catalan, Nature **538**, 219 (2016).
[7] A. Biancoli, C. M. Fancher, J. L. Jones, and D. Damjanovic, Nat. Mater. **14**, 224 (2015).
[8] X. Jiang, W. Huang, and S. Zhang, Nano Energy **2**, 1079 (2013).
[9] J. Harden, R. Teeling, J. T. Gleeson, S. Sprunt, and A. Jakli, Phys. Rev. E **78**, 31702 (2008).
[10] W. Ma and L. E. Cross, Appl. Phys. Lett. **86**, 72905 (2005).
[11] W. Ma and L. E. Cross, Appl. Phys. Lett. **81**, 3440 (2002).
[12] W. Ma and L. E. Cross, Appl. Phys. Lett. **88**, 2902 (2006).
[13] S. Zhang, X. Liang, M. Xu, B. Feng, and S. Shen, Appl. Phys. Lett. **107**, 142902 (2015).
[14] S. Baskaran, X. He, Y. Wang, and J. Y. Fu, J. Appl. Phys. **111**, 14109 (2012).
[15] W. Huang, K. Kim, S. Zhang, F. Yuan, and X. Jiang, Phys. Status Solidi (RRL)-Rapid Res. Lett. **5**, 350 (2011).
[16] G. Catalan, A. Lubk, A. H. G. Vlooswijk, E. Snoeck, C. Magen, A. Janssens, G. Rispens, G. Rijnders, D. H. A. Blank, and B. Noheda, Nat. Mater. **10**, 963 (2011).
[17] C. Liu and J. Wang, Theor. Appl. Mech. Lett. **7**, 88 (2017).
[18] S. Mathews, R. Ramesh, T. Venkatesan, and J. Benedetto, Science **276**, 238 (1997).

[19] A. Chanthbouala, A. Crassous, V. Garcia, K. Bouzehouane, S. Fusil, X. Moya, J. Allibe, B. Dlubak, J. Grollier, S. Xavier, C. Deranlot, A. Moshar, R. Proksch, N. D. Mathur, M. Bibes, and A. Barthélémy, Nat. Nanotechnol. **7**, 101 (2011).

[20] M. Bibes, Nat. Mater. **11**, 354 (2012).

[21] X. Yang, Z. Zhou, T. Nan, Y. Gao, G. M. Yang, M. Liu, and N. X. Sun, J. Mater. Chem. C **4**, 234 (2016).

[22] V. Garcia, S. Fusil, K. Bouzehouane, S. Enouz-Vedrenne, N. D. Mathur, A. Barthélémy, and M. Bibes, Nature **460**, 81 (2009).

[23] A. Gruverman, D. Wu, H. Lu, Y. Wang, H. W. Jang, C. M. Folkman, M. Y. Zhuravlev, D. Felker, M. Rzchowski, C.-B. Eom, and E. Y. Tsymbal, Nano Lett. **9**, 3539 (2009).

[24] H.-M. Yau, Z. Xi, X. Chen, Z. Wen, G. Wu, and J.-Y. Dai, Phys. Rev. B **95**, 214304 (2017).

[25] H. Zhou, J. Hong, Y. Zhang, F. Li, Y. Pei, and D. Fang, Phys. B Condens. Matter **407**, 3377 (2012).

[26] H. Zhou, J. Hong, Y. Zhang, F. Li, Y. Pei, and D. Fang, EPL (Europhysics Lett.) **99**, 47003 (2012).

[27] S. Huang, T. Kim, D. Hou, D. Cann, J. L. Jones, and X. Jiang, Appl. Phys. Lett. **110**, 222904 (2017).

[28] S. R. Kwon, W. Huang, L. Shu, F.-G. Yuan, J.-P. Maria, and X. Jiang, Appl. Phys. Lett. **105**, 142904 (2014).

[29] G. Catalan, L. J. Sinnamon, and J. M. Gregg, J. Phys. Condens. Matter **16**, 2253 (2004).